University of Nebraska - Lincoln
DigitalCommons@University of Nebraska - Lincoln

Biological Systems Engineering: Papers and Publications | Biological Systems Engineering

2011

Spatial Variability of Field Machinery Use and Efficiency

Viacheslav I. Adamchuk
University of Nebraska-Lincoln, viacheslav.adamchuk@mcgill.ca

Robert Grisso
Virginia Polytechnic Institute and State University, rgrisso@vt.edu

Michael F. Kocher
University of Nebraska-Lincoln, mkocher1@unl.edu

Follow this and additional works at: https://digitalcommons.unl.edu/biosysengfacpub

 Part of the Biological Engineering Commons

Adamchuk, Viacheslav I.; Grisso, Robert; and Kocher, Michael F., "Spatial Variability of Field Machinery Use and Efficiency" (2011). *Biological Systems Engineering: Papers and Publications*. 192.
https://digitalcommons.unl.edu/biosysengfacpub/192

This Article is brought to you for free and open access by the Biological Systems Engineering at DigitalCommons@University of Nebraska - Lincoln. It has been accepted for inclusion in Biological Systems Engineering: Papers and Publications by an authorized administrator of DigitalCommons@University of Nebraska - Lincoln.

Published (as Chapter 8) in *GIS Applications in Agriculture. Volume Two. Nutrient Management for Energy Efficiency,* D. E. Clay and J. F. Shanahan, eds. (Boca Raton, Florida: CRC Press, 2011), pp. 135-146.

Originally presented at the 2004 ASAE Annual International Meeting as Paper No. 041149.

Spatial Variability of Field Machinery Use and Efficiency

Viacheslav I. Adamchuk, Robert D. Grisso, and Michael F. Kocher

1 Executive Summary

In site-specific crop management, It is a common practice to log the geographic coordinates of agricultural machinery measured using a global satellite navigation system (GNSS) such as the global positioning system (GPS). Yield, fertilizer application, and seed placement maps provide useful data for making agronomic decisions. However, the travel path itself reveals valuable information about machinery performance. Often, during field operations, odd field shapes, obstacles, or contour farming will require operators to increase the complexity of the machinery maneuvering. This usually reduces field efficiency. This chapter presents a methodology to parameterize the spatially variable characteristics of traffic patterns, and to define field areas where field efficiency is significantly reduced. Geographic positions recorded during the harvesting of a field with a complex shape are provided to illustrate the method developed. The information obtained can be used to optimize traffic patterns, or to reevaluate the potential profitability of field areas that require different degrees of complexity in machinery maneuvering and therefore require varying energy use.

2 Introduction

Implementing precision agriculture practices in modern crop production generates a large volume of records containing the coordinates of the agricultural machinery's locations during various field operations. Historically, these coordinates were used to determine the location of the physical value associated with the corresponding field operation (i.e., crop yield, application or seeding rate, soil characterization, tractor performance, implement draft, etc.). Developing and processing numerous layers of spatial data has proven popular for making use of geographical coordinates. The log of the times and geographic coordinates of agricultural machinery within a field provides valuable information on machinery performance that can (and probably should) be used to determine the spatially variable cost of field operation. According to MAX® (Farming for MAXimum Efficiency, Conservation Technology Information Center, West Lafayette, IN), field operation costs can be as high as 25% of the total cost of crop production. Since field geometry frequently causes farmers to invest greater effort and time in operating within non-rectangular areas of the field (waterways, terraces, etc.), it can be misleading when developing profitability maps to assume a uniform distribution of machinery operation costs across the entire field area.

Field capacity (FC) (effective and theoretical) and field efficiency (FE) (ASABE, 2008a) are the primary parameters used to evaluate machinery performance. While FC represents the area of land processed per unit time for a particular field operation, FE is defined as the ratio between effective and theoretical field capacities and relates the estimated and actual time required to complete a field operation (with no reference to the area). In the past, field capacity or efficiency were evaluated only on a field basis, either by using machinery operation parameters or by simply using a reference table (ASABE, 2008b). For example, Renoll (1981) used a conventional recording method (a stop watch and a clipboard) to determine field machinery performance. Alternatively, Grisso et al. (2002) as well as Taylor et al. (2002) used records of machinery location determined with a GPS receiver. They proved geospatial field records to be an effective resource for evaluating overall machinery performance. In a study conducted by Grisso et al. (2004), the positions of agricultural machinery logged during harvesting and planting operations were used not only to evaluate FE but also to define parameters representing the complexity of traffic patterns. Steering angle, steering angle per distance traveled, steering rate, and radius of curvature were the primary indices introduced. Their field averages indicated some correlation with the overall FE when fields with various types of traffic patterns were analyzed.

The primary objective of this chapter is to present a methodology for using records of agricultural machinery positions and times to evaluate the spatial variability of machinery performance. Specifically, analytical tools are presented for the construction of spatial maps representing the variability of FE.

3 Methods

Several approaches are available for processing machinery position log files, including filters and geometrical transformations. However, in every case, the effi-

ciency of farm machinery operation can be affected by three factors: (1) the travel speed, (2) the effective swath width, and (3) the field traffic pattern. The position logging interval is assumed to be constant, but can affect the results reported as well. In this work, area coverage was used as the primary parameter in combining the three factors.

3.1 Algorithm Development

To develop an algorithm for traffic pattern processing, the following assumptions were made: first, that the entire log was created using a fixed time interval between successive machinery location coordinates (a logging option not always available); and second, that the resulting map should show the area coverage of the machine for every field location. It was also assumed that the coverage of farm machinery can be simplified using a sequence of rectangular segments defined by the recorded geographic positions. This is not the case when turning and the logging interval is relatively large. Figure 1 illustrates a route represented by four points: A, B, C, and D. Each segment of this route can be represented either as a sequence of rectangles with constant width (w) and variable distance (d), or as rectangles with constant width and fixed distance (d_f). The variable distance can be used to determine the actual coverage provided by the machine, and the fixed distance can be used to assess deviation from the theoretical coverage if a constant travel speed was maintained while operating along the same route. More complex segments incorporating travel pass curvature could also be used to better represent the actual coverage. In such a case, a minimum of three consecutive points would be used to estimate the radius of curvature and then determine the area of a sector of an annulus better representing the true ground coverage.

To assure that every field location has a defined coverage, an equally spaced grid with minimum and maximum coordinates corresponding to the endpoints of the field was used to construct the output. Figure 2 shows such a grid representing a section of a field with points corresponding to the machinery route A–B–C–D. Every linear segment (i.e., AB, BC, and CD) of the route was represented by the rectangular area coverage and was related to the grid cells overlapped by this rectangle. To illustrate the calculation procedure, a linear segment between points B (with

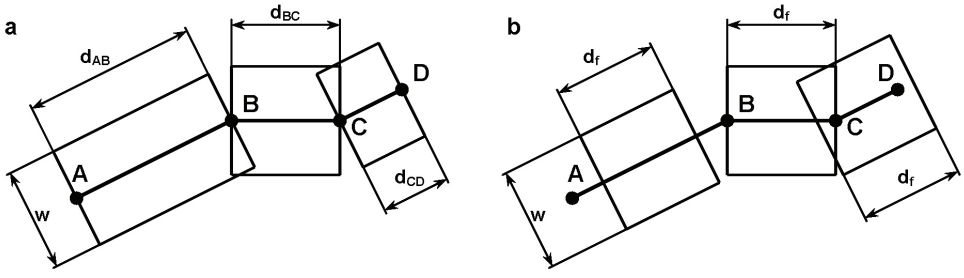

Figure 1. Simplified segments of equipment route ABCD using (a) variable (actual) travel speed and (b) constant (theoretical) speed of operation.

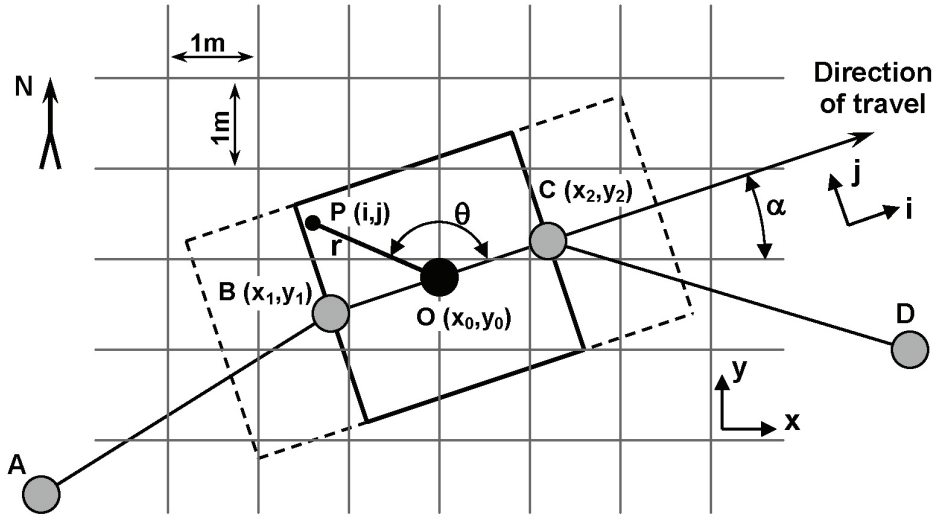

Figure 2. Area coverage computation diagram.

coordinates x_1, y_1) and C (with coordinates x_2, y_2) was considered. Values x and y corresponded to easting and northing coordinates, expressed in linear units (m). The simplified coverage segment was represented by a rectangle with width (w) corresponding to the physical width of the implement and the travel length (d) calculated as the distance between B and C:

$$d = \sqrt{(x_2 - x_1)^2 + (y_2 - y_1)^2} \tag{1}$$

The center of this rectangle $O(x_0, y_0)$ had coordinates

$$x_0 = \frac{x_1 + x_2}{2}, \quad y_0 = \frac{y_1 + y_2}{2} \tag{2}$$

By contrast, the same rectangular coverage area was viewed as an array of infinite points P with local coordinates i and j (Figure 2). It was assumed that the direction of i corresponded to the direction of travel and that for the center of rectangle O both i and j were equal to zero. Therefore, the i coordinate for point P ranged from $-d/2$ to $d/2$, and the j coordinate ranged from $-w/2$ to $w/2$. If the increments of the i and j coordinates are set to a finite number, a defined array of points $P(i, j)$ can be obtained. In this example, the increment for both coordinates was set 10 times smaller (0.1 m) than the side of a square grid cell (1 m). This allowed the total of $100 \times d \times w$ points P arranged in a $10d \times 10w$ array to represent the entire rectangle. Through a method illustrated in Figure 2, each point was assigned to the respective grid cells using x and y coordinates. This resulted in each of the $100 \times d \times w$ points P for a given rectangle being assigned to the respective grid cells covered by that rectangle. The number of points from the given rectangle that were within the boundaries of each grid cell, was added to the point total for that grid cell.

The (x, y) and (i, j) coordinate systems were related using the angle α between the travel direction and the positive x axis (true east):

$$\alpha = \begin{cases} \frac{\pi}{2} & \text{for } x_1 = x_2 \text{ and } y_1 < y_2 \\ \frac{3\pi}{2} & \text{for } x_1 = x_2 \text{ and } y_1 > y_2 \\ \tan^{-1}\left(\frac{y_2 - y_1}{x_2 - x_1}\right) & \text{for } x_1 < x_2 \\ \pi + \tan^{-1}\left(\frac{y_2 - y_1}{x_2 - x_1}\right) & \text{for } x_1 > x_2 \end{cases} \quad (3)$$

For cases in which both x and y coordinates remained the same between consecutive data records (e.g., stops), α values determined for the preceding records were used. In addition to the local rectangular coordinates i and j, every point P was defined using local polar coordinates r and θ with respect to the center of the rectangle O and the positive direction of i. This provided a relatively simple way to account for changes in travel direction for each new rectangle. Points with coordinates $i = 0$ or $j = 0$ were avoided to reduce the number of logical operators. Therefore

$$r = \sqrt{i^2 + j^2} \quad \text{and} \quad \theta = \begin{cases} \tan^{-1}\left(\frac{j}{i}\right) & \text{for } i > 0 \\ \pi + \tan^{-1}\left(\frac{j}{i}\right) & \text{for } i < 0 \end{cases} \quad (4)$$

To determine the grid cell coordinates (x, y) associated with a point $P(r, \theta)$, the following equations were used with values rounded to the nearest integer:

$$x = \text{round}(x_0 + r \cos(\theta + \alpha))$$

$$y = \text{round}(y_0 + r \sin(\theta + \alpha)) \quad (5)$$

After running the algorithm (Figure 3), a two-dimensional array Coverage 1 was obtained, with values corresponding to the percent coverage for each square meter of the field. This array represents the physical coverage of each grid cell, with greater than 100% coverage signifying more than $100 \times d \times w$ covered points P per grid cell (potential for overlaps) and less than 100% coverage indicating fewer than $100 \times d \times w$ covered points P per grid cell (skips). In contrast, the FE can be related to the coverage that would have been achieved if the travel speed remained constant across the entire field (Coverage 2). Therefore, a fixed (theoretical) distance be-

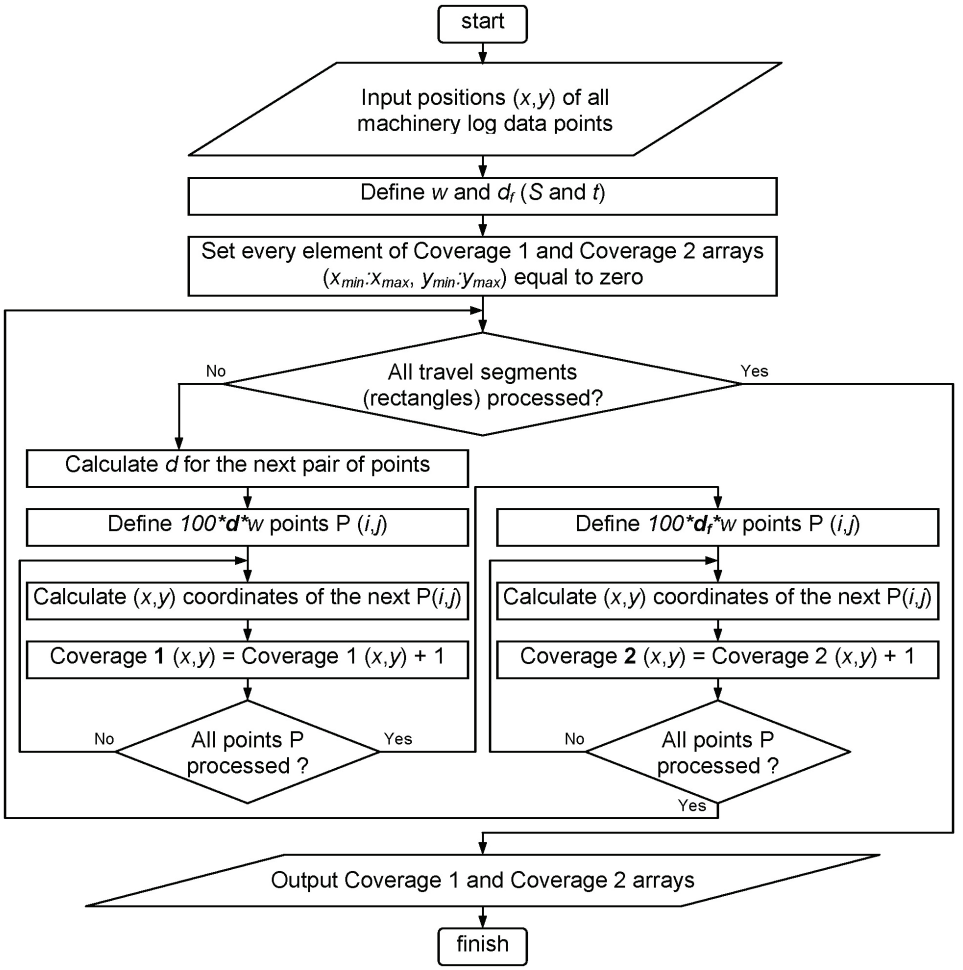

Figure 3. Algorithm for calculating Coverage 1 and 2 data layers.

tween two consecutive records (d_f), as shown in Figure 2, was defined as the product of the average operation travel speed (S), and the position logging interval (t):

$$d_f = S \cdot t \tag{6}$$

The described algorithm was executed using MATLAB® 2007a (The MathWorks, Natick, MA). The input delimited text file contained three columns (easting—x, northing—y, and time interval between two consecutive records). The output file had four columns containing the coordinates x and y for the center of each grid cell as well as the corresponding values for Coverage 1 and Coverage 2. Coverage 1 was calculated using the variable (actual) distance traveled d. The fixed (theoretical) distance (d_f) traveled was used in calculating the values corresponding to Coverage 2.

3.2 Supplemental Code

As long as the form of the delimited text data input remains unchanged, the supplemental *Efficiency count.m* script can be used to process and summarize an actual machinery travel log data set. The log file *Example.txt* contains three columns representing field easting and northing coordinates in meters (obtained through local projection of WGS-84 geographic coordinates with 10^{-6} degree resolution) as well as the log time interval in seconds. A zero value for the easting coordinate corresponds to the record for the western-most point of the field and a zero value for the northing coordinate corresponds to the record for the southern-most point in the field. Conversion of the GNSS coordinates to these local field coordinates was completed using Adamchuk (2001).

The output file *Example_count.txt* consists of five columns: (1) easting coordinate in meters for each 1 m^2 area of the field that has at least one coverage event, (2) the corresponding northing coordinate in meters, (3) the percent coverage according to the Coverage 1 layer, (4) the percent coverage according to the Coverage 2 layer, and (5) the percent coverage corresponding to complete stops only. Both the input and the output text files can be displayed within any geographic information system environment using an orthogonal projection, or after converting the local projection coordinates back to longitude and latitude, or using standard projections. If conventional projection method is applied to geographic coordinates in the input travel log file, geographic coordinates in the same projection will be used to generate the output file.

3.3 Example Field Data

To illustrate the algorithm output, an agricultural field with a complex shape (Field R1, Rogers Memorial Farm, Eagle, NE) with a total area of 4.24 ha was selected. A soybean harvesting operation was used in this example. The combine header was 4.6 m (15 ft) wide (w = 4.6 m). A total of 11.4 Mg of soybean (average yield of 2.69 Mg/ha) was harvested and removed from the field. The combine stopped and unloaded grain three times. Two data files were simultaneously generated. A PF3000™ (Ag Leader Technology, Inc., Ames, IA) yield monitor with an AgLeader Add-On GPS 3100 receiver (beacon differential correction) was used to collect yield data while harvesting. The position of the center of the combine was recorded in 4 s (0.25 Hz) intervals with the header down (during harvesting only). A standard begin/end of row delay filter was applied. In addition, a GPS 16 (Garmin International, Inc., Olathe, KS) receiver with Wide Area Augmentation System (WAAS) differential correction was placed 1.1 m to the right of the Ag Leader antenna. The receiver output was recorded independently in 1 s (1 Hz) intervals from the beginning to the end of field harvesting (including stops, maneuvering, and unloads).

Initial data processing included conversion of the geographic longitude and latitude into the local rectangular coordinates according to Adamchuk (2001), and correction of the position offset of the Garmin GPS 16 receiver. Figure 4 illustrates the nonstop position log (Garmin receiver at 1 Hz sampling rate) and positions recorded by the yield monitor (Ag Leader GPS receiver at 0.25 Hz sampling rate). The

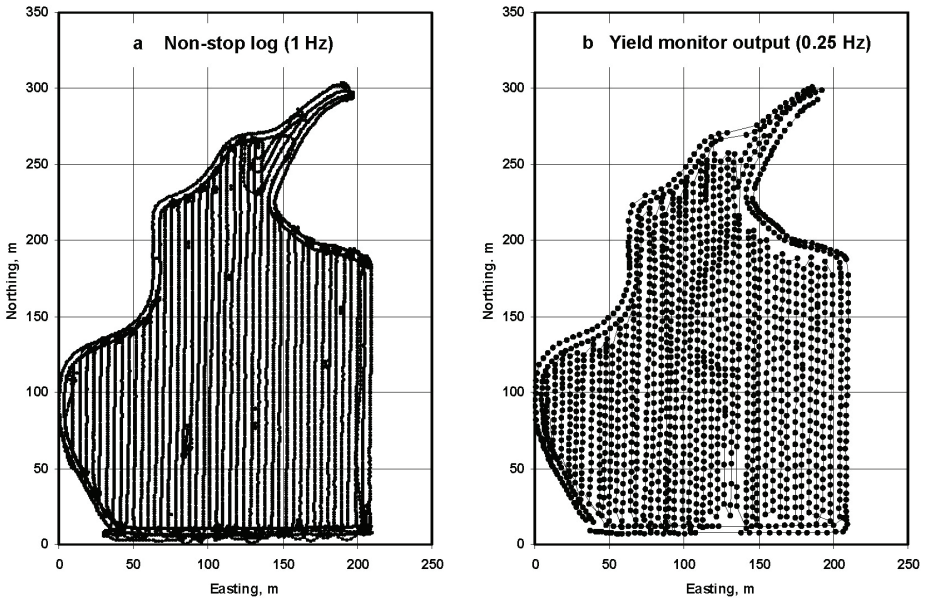

Figure 4. Combine positions logged (a) nonstop and (b) only while harvesting with the start and end of pass setting.

continuous log contained records from the beginning to the end of harvesting; the yield monitor output included harvesting locations only.

The algorithm developed can be applied to any logged travel route. However, the meaning of the Coverage 1 and 2 values will change depending on which positions are excluded from the input file. It is critical to identify whether or not turns, stops, and unexpected field maneuvering are included in the log file. In this study, the nonstop (1 Hz) log was used to analyze the spatial variability of the harvest efficiency. The yield monitor recordings were used primarily to define the average harvesting speed (S). Time gaps in the yield monitor recordings (times when the header was up so the combine was not engaged in harvesting the crop) were used to mark nonharvesting records in the nonstop (1 Hz) log. The non-harvesting records were ignored and the remaining speed data were averaged to determine the average harvesting speed, S. The average harvesting speed was 1.4 m/s, and, therefore, d_f = 1.4 m (for the continuous log in which t = 1 s).

The Coverage 1 and 2 maps reveal the spatial variability of the machinery performance. However, for decision making, this information should be converted into the conventional terms of effective capacity, field efficiency, and cost. From the overall evaluation of the recorded data, the field with an actual area of 4.24 ha was harvested in 2.78 h. This resulted in an effective field capacity (EFC) of 4.24 m^2/s (1.53 ha/h). On the other hand, the theoretical field capacity of the harvest operation (header width times average harvesting speed) was 6.44 m^2/s (2.32 ha/h). The ratio of the EFC to the theoretical field capacity (TFC) for the average speed of operation was 0.66. According to Jose and Brown (2002), $49.42/ha ($20/ac) is the most common farm custom rate for soybean harvesting. Therefore, the total cost of this operation was $210.

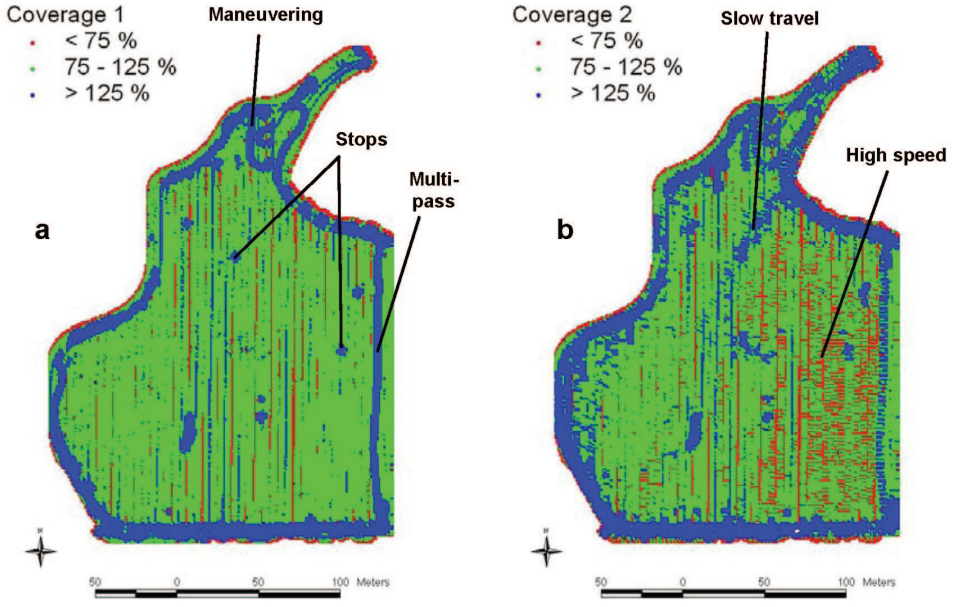

Figure 5. Grid of field coverage calculated using (a) variable (Coverage 1) and (b) fixed distances between consecutive points (Coverage 2).

Analysis of the algorithm outputs revealed that the sums of all nonzero grid cell point values from the Coverage 1 and 2 arrays were 5.80 and 6.42 ha, respectively. This means that the 37% increase in the Coverage 1 area compared to the actual area resulted from overlaps during maneuvering and reduced width of cut during harvest. In like manner, the 51% increase in the Coverage 2 area compared to the actual area was caused by both overlaps and overestimation of travel speed (including stops). The average travel speed (computed based on the entire nonstop data set) was 1.26 m/s (90% of the average harvesting speed). Therefore, the overall field efficiency of 0.66 (approximately equal to the ratio of actual field area to the Coverage 2 area) can be considered the product of the efficiency resulting from the combine route (e_{overlap} = actual field area/Coverage 1 area = 4.24/5.80 ha = 0.73) and the efficiency resulting from the inconsistent travel speed (e_{speed} = Coverage 1 area/Coverage 2 area = 5.80/6.42 ha = 0.90).

4 Results

Figure 5 shows spatial maps of Coverage 1 and 2 produced using the continuous log (Figure 4a). According to the color scheme, <75% coverage corresponds to the areas with incomplete coverage due to issues such as potential skips (Coverage 1 and 2) and operation at higher-than-average speed (Coverage 2). Similarly, >125% coverage indicates the potential for multiple coverage's due to overlaps, several passes, and stops (Coverage 1 and 2), and operation at lower-than-average speed (Coverage 2). The rest of the field shows areas with normal coverage (Coverage 1

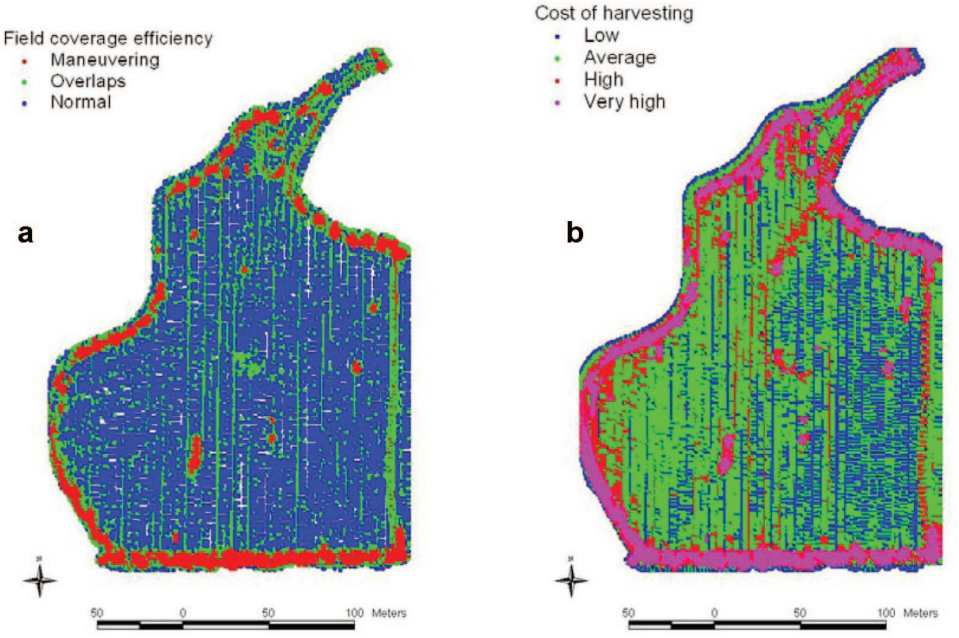

Figure 6. Categorized maps of (a) field coverage efficiency and (b) cost of harvesting. In (a), normal maneuvering is observed at 0.9–1.0, overlaps can be found at 0.5–0.9, and maneuvering corresponds to values below 0.5. In (b), low cost of harvesting is < $40/ha, medium is $40- 60/ha, high is $60–100/ha, and very high is > $100/ha.

and 2) and average harvesting speed (Coverage 2). The Coverage 1 map indicates the physical presence of the harvester. The Coverage 2 map also indicates areas where travel speed deviated from the average harvest speed. Since the size of a grid cell was 1 m^2 (less than the GPS receiver accuracy), some indications of potential skips and overlaps could result from the imprecise measurement of the harvester position. The rectangular representation of route segments between two consecutive points during high-speed turns might present additional noise. Map smoothing using conventional interpolation techniques (not presented) could improve the visual appearance of these maps.

Figure 6 shows categorical maps produced based on Coverage 1 and 2. A field coverage efficiency map (Figure 6a) was derived from Coverage 1 as the inverse of all grid cell point totals with higher than 100% coverage. It indicates coverage efficiency, which was categorized into three intervals: < 0.5 — excessive coverage for maneuvering; 0.5–0.9 — overlaps; and 0.9–1.0 — normal coverage. This map can be used to improve traffic patterns through optimization of the harvester route during non-harvest portions of the operation (unloads, turns, etc.).

Since the Coverage 2 map was developed based on the assumption of a constant speed, dividing its coverage values for each field location by the TFC resulted in the theoretical time spent in each field location. If time is used as the major indicator of investment (both labor and energy), the total cost of harvesting can be redistributed according to the time ($210 distributed over 2.78 h is equal to $0.021/s).

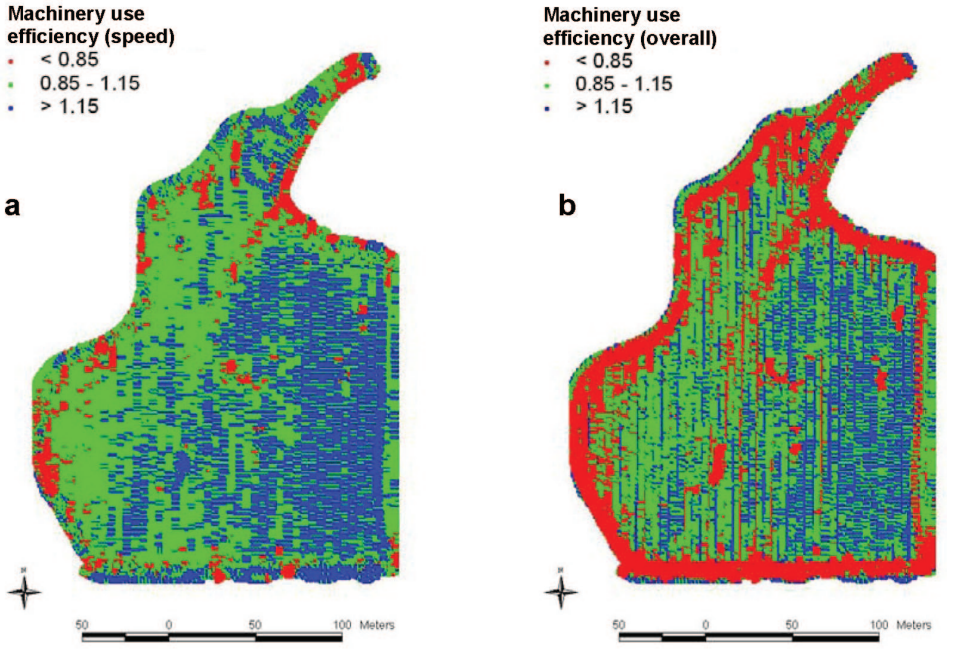

Figure 7. Machinery use efficiency maps representing (a) speed effect and (b) overall performance.

Figure 6b illustrates a cost of harvesting map categorized with < \$40/ha as the low cost, \$40–60/ha as average, \$60–100/ha as high, and > \$/100/ha as very costly harvesting. Conceptually, a yield map layer for each field operation could be used in conjunction with this kind of map to calculate an overall profitability map. If profit map values show losses or small gains in particular field areas (such as the northern portion of the illustrated field, Figure 6), alternative traffic patterns and/or land usage should be considered.

EFC and FE can be calculated to evaluate the overall performance of the operation as well as to investigate operational variation effects. Thus, Coverage 1 divided by the theoretical time (the same as the time used to calculate the cost of harvesting) corresponds to the physical coverage of each square grid area in a unit of time, or locally defined EFC. After dividing by the field average of these locally defined field capacity values (5.82 m^2/s or 2.10 ha/h), a map can be constructed showing relative machinery efficiency related to the variable speed effect (Figure 7a). Areas with a high speed of operation are represented with relative machinery efficiency values greater than 1 (more efficient than an average field location), while grid cells with relative machinery efficiency less than 1 showed the locations where the actual coverage area was smaller than what theoretically should have been covered using average TFC. This map removes most of the effects of maneuvering, and can be used to determine the locations of the actual slowdowns.

Overall machinery efficiency—the ratio between effective (area of a grid cell divided by time) and theoretical (6.44 m^2/s or 2.32 ha/h) field capacities—indicates the overall machinery performance efficiency (Figure 7b). This map relates to the

cost map and can be used to make judgments about operating in low-performing areas of the field (low efficiency and high cost). Although there are many ways to utilize these data layers, two major strategies can be pursued. The areas with relatively low machinery efficiency due to a systematic nonproductive machinery operation (involving extra turns, travel around obstacles, point rows, etc.) can be evaluated to determine more effective traffic patterns. And machinery efficiency expressed in energy use and/or monetary terms can be used to evaluate the spatial profitability while accounting for the inconsistent cost of field operations.

5 Conclusions

The maps presented in this work are examples of various types of information contained within the records of geographic positions logged during various field operations. The algorithm developed allows the producer to transform this information into two coverage maps (Coverage 1 and 2). The Coverage 1 map indicates field areas affected by repeated passes and variable true swath width. The Coverage 2 map shows the effect of variable travel speed as well. These generated maps can be converted into a set of data layers associated with conventional categories evaluating machinery performance (cost of operation, capacity, efficiency, etc.). These processed data layers will be complementary for decision-making strategies to improve site-specific crop management.

References

Adamchuk, V. I. Untangling the GPS data string. *Precision Agriculture Extension Circular EC 01-157.* Lincoln, NE: University of Nebraska Cooperative Extension, 2001.

ASABE Standards, 49th edn. S495.1 NOV2005. *Uniform Terminology for Agricultural Machinery Management.* St. Joseph, MI: ASABE, 2008a.

ASABE Standards, 49th edn. D497.5 FEB2006. *Agricultural Machinery Management Data.* St. Joseph, MI: ASABE, 2008b.

Grisso, R. D., Jasa, P. J., and Rolofson, D. Field efficiency determination from spatial data. *Applied Engineering in Agriculture* 18, 171 , 2002.

Grisso, R. D., Kocher, M. E, Adamchuk, V. I., Jasa, P. J. , and Schroeder, M. A. Field efficiency determination using traffic pattern indices. *Applied Engineering in Agriculture* 20, 563, 2004.

Jose, H. D. and Brown, L. J. Nebraska farm custom rates: Part II. *Extension Circular EC02-826-A.* Lincoln, NE: University of Nebraska Cooperative Extension, 2002.

Renoll, E. S. Predicting machine field capacity for specific field and operating conditions. *Transactions of the ASAE* 24, 45, 1981.

Taylor, R. K., Schrock, M. D., and Staggenborg, S. A. *Extracting Machinery Management Information from GPS Data.* Paper No. 02-10008. St. Joseph, MI: ASAE, 2002.